Journal of Materials Chemistry

Dynamic Article Links

Cite this: J. Mater. Chem., 2012, 22, 7609

www.rsc.org/materials

PAPER

Optically switchable photonic crystals based on inverse opals partially infiltrated by photoresponsive liquid crystals

Yan Jun Liu,*[a] Zhongyu Cai,[b] Eunice S. P. Leong,[a] Xiu Song Zhao*[c] and Jing Hua Teng*[a]

Received 21st November 2011, Accepted 10th February 2012
DOI: 10.1039/c2jm16050a

We demonstrate optically switchable photonic crystals based on SiO_2 inverse opals infiltrated with photoresponsive liquid crystals. The optical properties of the hybrid organic/inorganic structure were characterized by measuring reflectance spectra. The Bragg reflection of the photonic crystal, *i.e.* photonic band gap, can be switched upon UV photoirradiation. The physical mechanism underlying this switchable behavior is the nematic–isotropic phase transition of the liquid crystals inside the opals triggered by the *trans–cis* isomerization of the photochromic liquid crystal molecules, resulting in a change of the refractive index contrast between the liquid crystal and the SiO_2 inverse opal. The experimental results are in excellent agreement with the analytical calculations. With advantages in cost-effective fabrication, easy integration, and all-optical control, this kind of photonic crystals could find many active photonic applications.

Introduction

Photonic crystals (PhCs) or photonic bandgap (PBG) materials[1,2] hold promise for an emerging generation of nano- and mesoscale optoelectronic components. Many potential applications of PhCs require the capability to actively control the band structure through external stimuli. The characteristics of a PBG structure mainly depend on the lattice constants and the refractive index contrast of the constructing dielectric materials. Therefore, the PBG tuning can be achieved by controlling either the lattice constant or refractive index. Thus far, various approaches have been exploited to tune the PBG, including the volume phase transition of hydrogels by controlling the temperature, the pH, and the ionic state,[3–5] mechanical deformation,[6] magnetically induced particle motion,[7,8] chemical swelling,[9] the electro-optic effect of ferroelectrics,[10] temperature controlled dopant solubility in liquid crystal,[11] thermally/optically induced phase transition of liquid crystal,[12,13] electrically controlled birefringence of liquid crystal,[14–17] and liquid mixture imbibitions.[18] Among these approaches, all-optical control stands out since it leverages the benefits of light directed effects—remote, temporal, and spatial control.

To realize photoactive PhCs, one may utilize the photoswitching effects of photoresponsive dyes, *e.g.*, azobenzene derivatives. The reversible *trans–cis* isomerization of azobenzene derivatives by photoirradiation is the root of all-optical control.[19] This isomerization process can also induce the reorientation of liquid crystal molecules.[20] Recently, we have reported optically switchable gratings (one-dimensional PhCs) based on azo-dye-doped holographic polymer-dispersed liquid crystals (HPDLCs).[21] All-optical switching in photonic structures based on photochromic LCs has also been demonstrated.[22–25] However, the switching performance is relatively poor due to two main reasons: (1) high surface-to-volume ratio induced strong anchoring strength; (2) non-uniform distribution of LC droplets size. A delicate design of the photonic structures is desired to confine the LCs with relatively low anchoring energy and uniform droplet size, thus enhancing the switching performance.

Synthetic inverse opals meet this requirement to a large extent since they have uniform and periodical spheroidal voids with flexible control of size. An inverse opal possesses a directional PBG along the densest closely packed Γ–L direction, [111], which can be experimentally characterized by a strong Bragg reflectance peak or transmission dip. Moreover, fabrication of inverse opals is simple and cost-effective. Demonstrating a PBG in visible range requires the void size to be larger than 200 nm in diameter, which is much larger than the LC droplet size (less than 100 nm in diameter) in HPDLCs. Upon LC infiltration, the large voids could provide relatively low surface-to-volume ratio, hence decreasing the anchoring strength of LCs. More importantly, the effective refractive index of the opal structure can be controlled by the LC infiltration to tune the Bragg reflection since the LC possesses a birefringence, Δn_{LC}. The refractive index of LCs can be tuned between the ordinary (n_o) and the extraordinary (n_e) index values by properly controlling the orientation of the LC director. So far, LC-infiltrated inverse opals have extensively

[a]*Institute of Materials Research and Engineering, Agency for Science Technology and Research (A*STAR), 3 Research Link, Singapore 117602, Singapore. E-mail: liuy@imre.a-star.edu.sg; jh-teng@imre.a-star.edu.sg*
[b]*Department of Chemical and Biomolecular Engineering, National University of Singapore, 4 Engineering Drive 4, Singapore 117576, Singapore*
[c]*School of Chemical Engineering, Faculty of Engineering, Architecture and Information Technology, The University of Queensland, St Lucia, Brisbane, QLD 4072, Australia. E-mail: george.zhao@uq.edu.au*

been studied but all are based on complete infiltration.[26–29] In this paper, we report an optically switchable photonic crystal based on an SiO_2 inverse opal partially infiltrated by photoresponsive LCs. We observed different phenomena with the completely infiltrated case. The underlying mechanism is analyzed. The partial infiltration could provide an additional degree of freedom to control the desired Bragg reflection in a wide range.

Experimental

Chemicals

All chemicals, including styrene (99%, Aldrich), potassium persulfate (99%, Aldrich), ethanol (99.95%, Aldrich), sulfuric acid (98%, Merck), hydrogen peroxide (H_2O_2, 35%, Scharlau Chemie S.A.), tetraorthosilicate (TEOS, 98%, Aldrich), and hydrochloric acid (37%, Sigma-Aldrich), were used as purchased. Microscope cover glasses (22 mm × 22 mm × 0.3 mm, Deckgläser) were used as substrate for the fabrication of crack-free SiO_2 inverse opals. The glass substrate was treated in a piranha solution (3 : 1 v/v 98% H_2SO_4/35% H_2O_2) at 60 °C for 2 h before use.

Fabrication of silica inverse opals

According to the work of Wang and Zhao,[30] the fabrication of SiO_2 inverse opals was conducted in two sequential steps: (a) convective self-assembly of polystyrene (PS)/SiO_2 colloidal crystals and (b) calcination of the samples to remove PS (Fig. 1). The PS spheres were synthesized using a surfactant-free emulsion polymerization method,[31] which had a diameter of 277 nm. A standard TEOS sol consisting of TEOS, ethanol (100%) and 0.10 M HCl with the ratio of 1 : 2 : 1 by weight was prepared. Prior to use, a vial containing the colloid/TEOS suspension was sonicated for 30 min. The PS/SiO_2 composite colloidal crystal films were fabricated by adding a 4.39 vol% PS colloidal suspension (284.6 μL) to the mixture of deionized H_2O (10 mL) and standard hydrolyzed TEOS solution (90 μL). A glass substrate was then placed vertically in the vial. The solvent was evaporated over a period of 1–2 days in an oven at 65 °C to allow the deposition of thin colloidal crystal films on the substrate. The films were then calcined in air at 450 °C (~2 °C min^{-1}) for ~4 h to completely remove the PS microspheres and partially sinter the SiO_2 matrix.

Liquid crystal infiltration

The photoresponsive LCs consisted of 87.3 wt% nematic LC, E7 (Merck) and 12.7 wt% photochromic LC, 4-butyl-4-methyoxyazobenzene (BMAB), which were physically mixed at an elevated temperature of 80 °C to form a homogeneous mixture. The mixed LCs were spin-coated (3000 rpm) onto the SiO_2 inverse opals and then infiltrated into the voids of the inverse opals based on capillary forces. Note that the LCs were heated to keep the isotropic phase in order to ease the infiltration. When the rodlike *trans*-isomer of BMAB absorbs the UV light, it triggers a reversible conformational change to the kinked, *cis*, state. The *cis*-isomer affects the host nematic as an impurity, disrupting the local order and lowering the clearing temperature. This order change generates a photoinduced refractive index modulation.

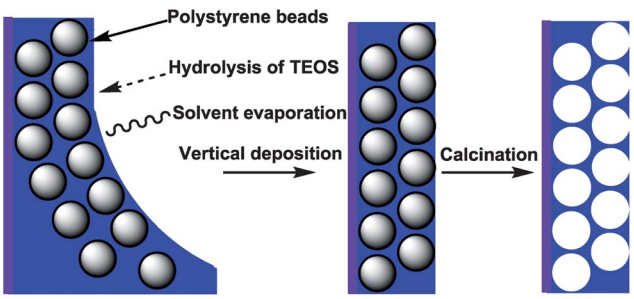

Fig. 1 Schematic showing the fabrication process of SiO_2 inverse opals.

Measurement of optical spectra

Optical reflection spectra were measured with an unpolarized probe light beam using a UV-Vis-NIR microspectrophotometer (CRAIC QDI 2010™). The probe light beam was focused to have a detecting area of 7.1 × 7.1 μm^2 using a 36× objective lens combined with a variable aperture. The dynamic spectral change was achieved when the hybrid organic/inorganic structure was subject to a flood exposure using a UV light source (ELC-410).

Results and discussion

Fig. 2a and b respectively show the top and cross-sectional views of the SiO_2 inverse opal after calcination. It can be seen from Fig. 2a that the diameter of the spheroidal voids is ~230 nm. Comparing to the PS spheres used in the experiment, there was a substantial decrease (17%) in diameter for the spheroidal voids due to the calcination of PS spheres. After inversion, the resulted filling ratio of the spheroidal voids was estimated to be ~68%.

Fig. 3 shows the measured reflection spectra before and after LC infiltration for the SiO_2 inverse opals. Before LC infiltration, the SiO_2 inverse opals showed a Bragg reflection peak at 376 nm and exhibited a full-width at half-maximum (FWHM) of 49 nm (13.0%). Upon LC infiltration, the reflection peak red-shifted from 376 nm to 410 nm with a smaller FWHM of 21 nm (5.2%). The red-shift was attributed to the increase in the average refractive index of the film and the decrease in FWHM to the lower dielectric contrast that resulted from the partial replacement of air with LCs. Moreover, there is a significant decrease in reflectance due to the decreased refractive index contrast for the LC-infiltrated case, which agrees with the expectation that the Bragg reflection peak collapses when the effective refractive indices between the spheroidal voids and SiO_2 match each other. It is worth mentioning that the background wavy spectra observed from SiO_2 inverse and LC-infiltrated opals are attributed to Fabry–Pérot interference in the thin film, that is, interference between the multiple reflections of light between the two reflecting surfaces (air–film and air–substrate interfaces).[32]

For closely packed face-centered cubic (FCC) PhCs under normally incident probe light, the Bragg reflectance peak results from the first order diffraction from the (111) planes of the opal structures, which corresponds to the PBG between the second and third bands along the Γ–L direction in reciprocal space. The reflectance peak for the (111) plane of an FCC lattice can be analytically determined by Bragg's law,[33] as follows:

$$\lambda = 2d_{111}[n_p^2\phi + n_m^2(1 - \phi)]^{1/2} \quad (1)$$

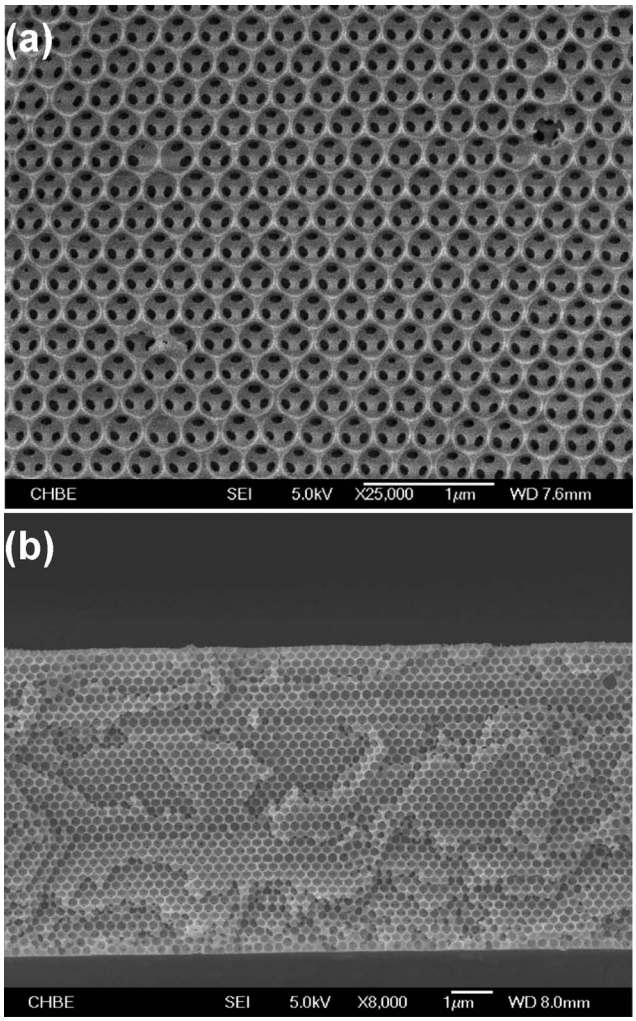

Fig. 2 SEM images showing top (a) and cross-sectional (b) views of the SiO_2 inverse opals.

where d_{111} is the lattice spacing, ϕ is the particle volume fraction, n_p and n_m are the refractive indices of the particles and the surrounding medium, respectively.

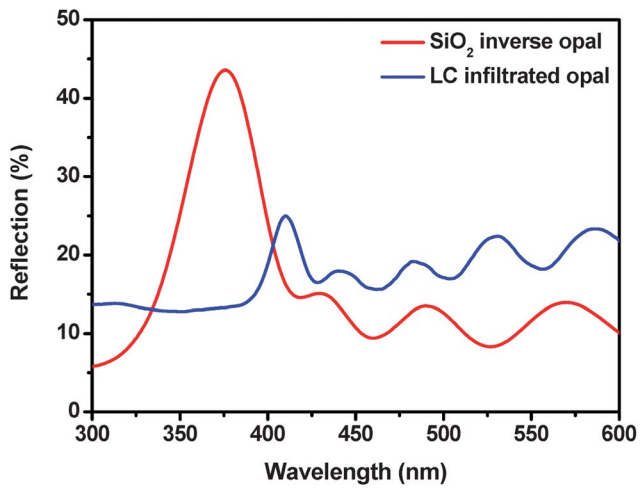

Fig. 3 Reflection spectra before and after LC infiltration. The peaks indicate the Bragg reflection.

An incomplete infiltration of LCs inside the spheroidal voids was confirmed by comparing the red-shift from experimental (34 nm) and calculated (124 nm by supposing complete infiltration with $n_{SiO_2} = 1.47$ and $n_{LC} = 1.6$) results from eqn (1). For the incomplete infiltration, the effective refractive index can be written as

$$n_{eff} = \left[\phi_{SiO_2} n_{SiO_2}^2 + \phi_{LC} n_{LC}^2 + (1 - \phi_{SiO_2} - \phi_{LC}) n_{air}^2\right]^{1/2} \quad (2)$$

By fitting the peak position according to the volume filling fraction, only about ~14% LCs are infiltrated inside the voids and take account in shifting the reflection peak. We believe that the incomplete infiltration was attributed to the small LC volume, which was controlled by the spin speed.

For the azo-dye-doped optical materials, a distinct advantage is that they can be optically controlled, an important factor in the future development of all-optical devices. Fig. 4 shows the changes in reflectance of LC-infiltrated inverse opals under different pumping intensities. With the pumping intensity increasing from 0 to 40 mW cm^{-2}, the reflection peak became much flatter, indicating decreased diffraction; meanwhile, the reflection peak demonstrated ~4 nm blue-shift, indicating increased index modulation. In addition, the reflection in the whole band decreased, which could be attributed to the decreased transmission through the thin top LC layer. Fig. 5 shows the time-dependent response of the PhCs under different pumping intensities (10, 22.5, and 40 mW cm^{-2}). When the pumping intensity was increased, the rising time ("ON" process) became faster, while the falling time ("OFF" process) is a self-relaxation process, which is more dependent on the material properties.

We note that Kubo *et al.* have reported optical switching from similar LC-infiltrated inverse opals completely infiltrated with photoresponsive LCs.[27,28] They observed that when a pumping light was on, the reflection peak appeared, corresponding to the aforementioned PBG; in contrast, we observed that the reflection peak decreased. We believe that this discrepancy was due to the difference in the LC alignment inside the spheroidal voids. In their work, they proposed that the LC molecules in the nematic phase are aligned parallel to the void surfaces (known as bipolar structure) for the completely infiltrated spheroidal voids

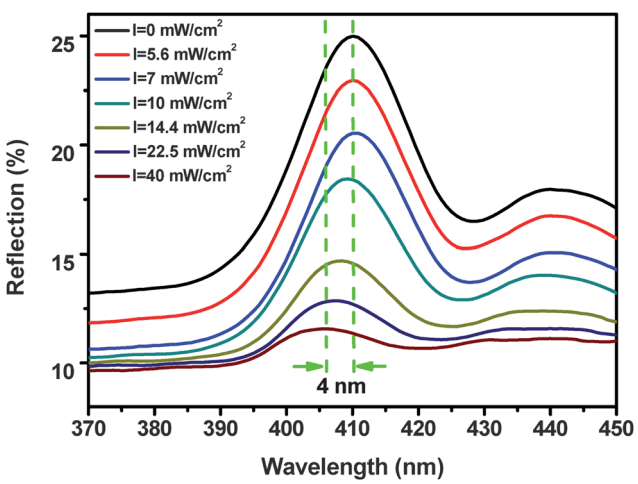

Fig. 4 Reflection spectra measured at different pumping intensities.

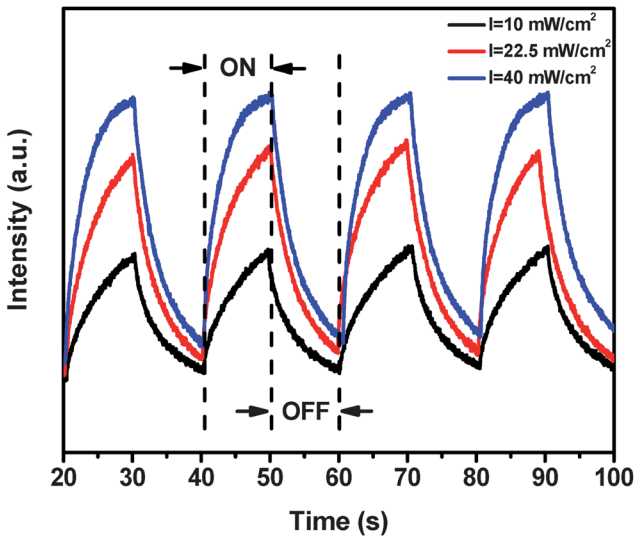

Fig. 5 Photoresponse of the LC-infiltrated SiO_2 inverse opal at different pumping intensities. The "ON" and "OFF" processes are labeled.

(Fig. 6a). However, the orientation of the polar axes of the bipolar structure of LC in different spheroidal voids is totally random, showing a macroscopically isotropic state. In our case, since the spheroidal voids were not fully infiltrated, the infiltrated LCs were located at the bottom of the voids by gravity (Fig. 6b). Although the same alignment principle of the LC molecules still applies to our case, the orientation of the polar axes of the bipolar structure of LC in different spheroidal voids is totally identical, showing a macroscopically nematic state. When the pumping UV light was on, the BMAB molecules absorbed the UV light and transformed from *trans* to *cis*, inducing the phase transition of the LCs from nematic to isotropic. The empirical effective index for a nematic and isotropic LC layer can be estimated to be $n_{nem} \cong [(n_o^2 + n_e^2)/2]^{1/2}$ and $n_{iso} \cong (2n_o + n_e)/3$, respectively. For the LC E7 used in our experiment, these values are $n_{nem} = 1.710$ and $n_{iso} = 1.654$ (@ $\lambda = 400$ nm and 25 °C). The refractive index of SiO_2 is $n_{SiO_2} \cong 1.470$. From eqn (1) and (2), the calculated reflection peaks at both nematic and isotropic phases for the LC-infiltrated case are about 411 nm and 407 nm, respectively, which is in excellent agreement with the experimental data. For azo-dyes, after removing the light pump, the *cis*-form goes back to the *trans*-form through a thermal relaxation process or a visible light, which indicates that the optical switching behaviour is reversible, as shown in Fig. 5.

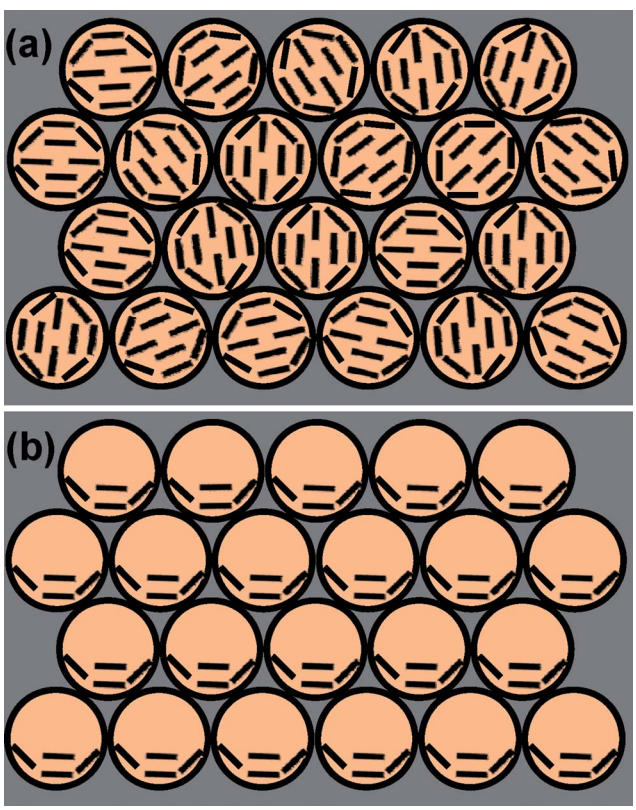

Fig. 6 Models of the orientation of LC molecules for the completely (a) and partially (b) infiltrated spheroidal voids in inverse opal film. The short lines in the circles represent the orientation of the LCs.

Conclusions

We have demonstrated optically switchable photonic crystals based on SiO_2 inverse opals partially infiltrated by photoresponsive LCs. A macroscopically nematic state of LCs was shown in the partially LC-infiltrated inverse opals. Upon UV photoirradiation, the Bragg reflection peak was switched off. The *trans–cis* photoisomerization-induced N–I phase transition of the LCs accounted for the switching of Bragg reflection. With the advantages of cost-effective fabrication, easy integration, and all-optical control, this kind of PhCs offers many possibilities in active photonic and plasmonic devices.

Acknowledgements

This work was financially supported by Agency for Science, Technology and Research (A*STAR), under grant no. 0921540099 and 0921540098. X. S. Zhao also thanks the Australian Research Council (ARC) for the financial support of this work under the ARC Future Fellow Program (FT100100879).

Notes and references

1 E. Yablonovitch, *Phys. Rev. Lett.*, 1987, **58**, 2059.
2 S. John, *Phys. Rev. Lett.*, 1987, **58**, 2486.
3 J. H. Holtz and S. A. Asher, *Nature*, 1997, **389**, 829.
4 J. M. Weissman, H. B. Sunkara, A. S. Tse and S. A. Asher, *Science*, 1996, **274**, 959.
5 K. Lee and S. A. Asher, *J. Am. Chem. Soc.*, 2000, **122**, 9534.
6 K. Yoshino, Y. Kawagishi, M. Ozaki and A. Kose, *Jpn. J. Appl. Phys.*, 1999, **38**, L786.
7 X. Xu, G. Friedman, K. D. Humfeld, S. A. Majetich and S. A. Asher, *Chem. Mater.*, 2002, **14**, 1249.
8 H. Kim, J. Ge, J. Kim, S. Choi, H. Lee, H. Lee, W. Park, Y. Yin and S. Kwon, *Nat. Photonics*, 2009, **3**, 534.
9 H. Fudouzi and Y. Xia, *Langmuir*, 2003, **19**, 9653.
10 B. Li, J. Zhou, L. Li, X. J. Wang, X. H. Liu and J. Zi, *Appl. Phys. Lett.*, 2003, **83**, 4704.
11 Y. Huang, Y. Zhou, C. Doyle and S. T. Wu, *Opt. Express*, 2006, **14**, 1236.
12 K. Yoshino, Y. Shimoda, Y. Kawagishi, K. Nakayama and M. Ozaki, *Appl. Phys. Lett.*, 1999, **75**, 932.
13 M. Kamenjicki, I. K. Lednev and S. A. Asher, *J. Phys. Chem. B*, 2004, **108**, 12637.
14 Y. Shimoda, M. Ozaki and K. Yoshino, *Appl. Phys. Lett.*, 2001, **79**, 3627.
15 Y. J. Liu and X. W. Sun, *Appl. Phys. Lett.*, 2006, **89**, 171101.

16 Y. J. Liu and X. W. Sun, *Jpn. J. Appl. Phys.*, 2007, **46**, 6634.
17 Y. J. Liu, H. T. Dai, E. S. P. Leong, J. H. Teng and X. W. Sun, *Appl. Phys. B: Lasers Opt.*, 2011, **104**, 659.
18 J. Li, W. Huang and Y. Han, *Colloids Surf., A*, 2006, **279**, 213.
19 Y. J. Liu, H. T. Dai and X. W. Sun, *J. Mater. Chem.*, 2011, **21**, 2982.
20 K. Ichimura, *Chem. Rev.*, 2000, **100**, 1847.
21 Y. J. Liu, Y. B. Zheng, J. Shi, H. Huang, T. R. Walker and T. J. Huang, *Opt. Lett.*, 2009, **34**, 2351.
22 A. Urbas, V. Tondiglia, L. Natarajan, R. Sutherland, H. Yu, J.-H. Li and T. J. Bunning, *J. Am. Chem. Soc.*, 2004, **126**, 13580.
23 L. De Sio, S. Serak, N. Tabiryan, S. Ferjani, A. Veltri and C. Umeton, *Adv. Mater.*, 2010, **22**, 2316.
24 L. De Sio, S. Serak, N. Tabiryan and C. Umeton, *J. Mater. Chem.*, 2011, **21**, 6811.
25 V. K. S. Hsiao and W.-T. Chang, *Appl. Phys. B: Lasers Opt.*, 2010, **100**, 539.
26 K. Busch and S. John, *Phys. Rev. Lett.*, 1999, **83**, 967.
27 S. Kubo, Z.-Z. Gu, K. Takahashi, Y. Ohko, O. Sato and A. Fujishima, *J. Am. Chem. Soc.*, 2002, **124**, 10950.
28 S. Kubo, Z.-Z. Gu, K. Takahashi, A. Fujishima, H. Segawa and O. Sato, *J. Am. Chem. Soc.*, 2004, **126**, 8314.
29 E. Graugnard, S. N. Dunham, J. S. King, D. Lorang, S. Jain and C. J. Summers, *Appl. Phys. Lett.*, 2007, **91**, 111101.
30 L. Wang and X. S. Zhao, *J. Phys. Chem. C*, 2007, **111**, 8538.
31 S.-E. Shim, Y.-J. Cha, J.-M. Byun and S. Choe, *J. Appl. Polym. Sci.*, 1999, **71**, 2259.
32 E. Hecht and A. Zajac, *Optics*, Addison Wesley, USA, 4th edn, 2002.
33 S. H. Park and Y. Xia, *Langmuir*, 1999, **15**, 266.